Piezoelectric Sensor for Acoustic Wave Detection in Anisotropic Systems

G. A. Barbosa[1], S. Lanceros-Mendez[2], J. Campos[2], J. Pamplona[3], M. Zamith[2],
A. M. Almeida[2], J. M. Cabral[1] and J. G. Rocha[1,*]
[1]Industrial Electronics Dept., University of Minho, Campus de Azurem, 4800-058 Guimaraes, Portugal
[2]Physics Dept., University of Minho, Campus de Gualtar, 4700-053 Braga, Portugal
[3]Earth Sciences Dept., University of Minho, Campus de Gualtar, 4700-053 Braga, Portugal
[*]gerardo@dei.uminho.pt

***Abstract*-This paper describes a seismic wave sensor, its readout electronics and data acquisition system. The seismic sensor is based on piezoelectric materials, which show the ability of transforming mechanical into electrical signals. In particular, the present sensor is based on a piezoelectric polymer, poly(vinilidene fluoride) as its main characteristics made it suitable for detecting the amplitude and frequencies involved in seismic events. After a general background on seismic events, waves and piezoelectric materials, the main steps on the sensor design and fabrication, the data acquisition system and the first test results are presented.**

I. INTRODUCTION

Earthquakes occur due to a sudden release of energy stored in the crust of the earth. This energy release may come from a slippage along a geologic fault or from a magma movement associated with volcanic activity. This sudden motion causes the generation of seismic waves that propagate through the earth from its point of origin, called the focus. A seismic wave is simply a way of transferring energy from one point to another within the earth. The focus corresponds to the place where the energy is released, while the epicenter corresponds to the point of the earth's surface directly above the focus.

When an earthquake occurs, several kinds of waves are produced with different frequencies and propagation speeds, which depend on the properties of the Earth composition at a given point. The waves, which spread in different types of rocks and in the Earth surface, are subject to reflection and refraction phenomena. These phenomena can lead to wave amplification and the consequently increase of the destruction potential.

The reflected seismic energy is never the first one that arrives, and therefore must be identified in a usually complex set of overlapping seismic arrivals. The field and processing time for a given linear footage of seismic reflection survey are much greater than for seismic refraction. Seismic reflection can be performed in the presence of low velocity zones or velocity inversions, generally has a lateral resolution higher than the seismic refraction, and can delineate very deep density contrasts with much less shot energy and shorter line lengths than would be required for a comparable refraction survey depth.

A wave is considered transverse when the disturbance is perpendicular to the propagation direction, as it happens in a vibration of a rope. If a rope is tied to a wall and in the other end an up and down movement is performed, the verified oscillation is a transverse wave. Fig. 1 shows an example of transverse seismic wave, also called s-wave.

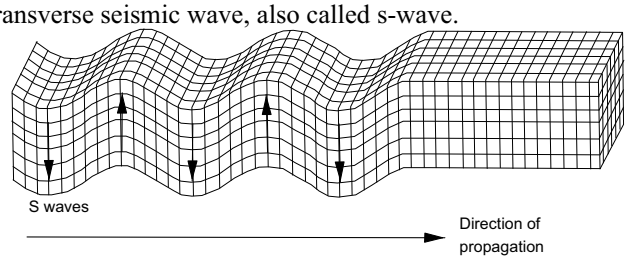

Fig. 1. Propagation of a transverse, secondary or s wave.

When the disturbance is parallel to the direction of propagation, the wave is classified as longitudinal wave. If a spring is compressed and stretched, the disturbance is parallel to the direction of propagation, so the generated wave is longitudinal, or p-wave (Fig. 2).

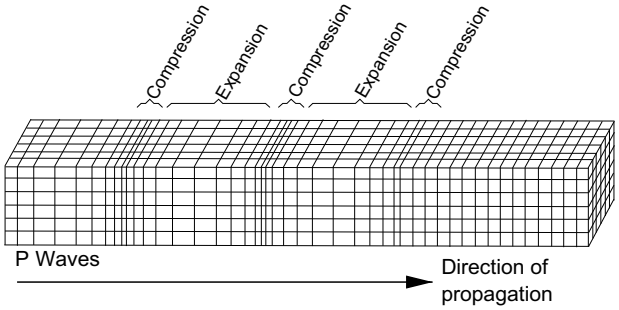

Fig. 2. Propagation of a longitudinal, primary or p wave.

The main goal of this work is to measure the amplitude and frequency of the sound waves caused by seismic events that propagate trough the earth, at higher frequencies than the conventional ones. The conventional seismic sensors usually cover a frequency range from tenths to hundreds of Hz [1]. Our main goal is to develop a sensor and the respective readout unit capable to operate in a frequency range up to 50 kHz.

II. BACKGROUND

A. Mechanical wave sensors

The mechanical wave transducers are devices that transform vibration energy into electrical energy. They can be

classified as electrostatic, electromagnetic or piezoelectric transducers, according to their working principle (here we disregard the indirect mechanical vibration sensors like the ones based on optical principles). For the present work, we will use piezoelectric sensors. The main reasons for this choice will be presented later in this article.

In 1880, Jacques and Pierre Curie discovered an unusual characteristic of certain crystalline minerals: when subjected to a mechanical force, the crystals became electrically polarized [3]. The effect is known as piezoelectricity. Nowadays, the piezoelectric materials (crystals, ceramics and polymers) are quite known and often used in several applications.

The conversion of electrical impulses into mechanical vibrations and the conversion of mechanical vibrations into electrical energy is the basis for testing mechanical waves using an active element that consists in a piece of polarized material with electrodes attached to two of its opposite faces [4].

The active element of most transducers used today is a traditional piezoelectric ceramic containing perovskite crystals, each consisting in a small, tetravalent metal ion, usually titanium or zirconium, in a lattice of larger bivalent metal ions, usually lead or barium, and O2- ions. Under conditions that confer tetragonal or rhombohedral symmetry, each crystal has a dipole momentum. The existence of this dipole causes a crystalline structure deformation in the presence of an electric field and vice-versa, that is, it produces an electric field variation when subjected to a mechanical deformation.

The phenomenon of piezoelectric effect discovered by the Curie brothers is based on the variation of the physical dimensions of certain materials subject to electric fields, and vice-versa. When these materials suffer a force F, they develop an electrical potential difference or voltage. This phenomenon is called direct piezoelectric effect. If there is no force or any kind of acceleration, the voltage across the piezoelectric element is null, but if a pressure is applied, the changes in the dimensions of the piezoelectric element are translated into electrical voltage changes.

When an electric voltage change is applied to a piezoelectric material, it shows a deformation. Changing voltage polarity at its electrode terminals, the crystal gets shorter or fatter. This phenomenon is called inverse piezoelectric effect.

III. SENSOR THEORY

The electromechanical cross coupling of piezoelectric materials is usually described by two constitutive equations:

$$P_m = d_{mi}\sigma_i + \chi_{ik}^{\sigma} E_k, \tag{2}$$

which describes the direct piezoelectric effect, and

$$\varepsilon_i = S_{ij}^{E}\sigma_j + d_{mi}E_m, \tag{3}$$

which describes the inverse piezoelectric effect, where P is the electric displacement (polarization), d is the piezoelectric tensor, σ is the applied stress, χ is the permittivity, E is the applied electric field, ε is the strain, S is the compliance coefficient tensor. The subscripts i, j = 1, 2, 3, 4, 5, 6 and k, m = 1, 2, 3, denote the direction to which the physical properties are related, which correspond to:

1 – direction of stretching of the film;

2 – direction in the plane of stretching, perpendicular to 1;

3 – direction of polarization (perpendicular to the plane 1,2);

4 – rotation in the plane 2,3;

5 – rotation in the plane 1,3;

6 – rotation in the plane 1,2.

The superscript σ in χ denotes the permittivity at constant strain and the superscript E in S denotes the compliance at constant electric field.

Tensor d can be written in the matrix form as:

$$d = \begin{bmatrix} 0 & 0 & 0 & 0 & d_{15} & 0 \\ 0 & 0 & 0 & d_{24} & 0 & 0 \\ d_{31} & d_{32} & d_{33} & 0 & 0 & 0 \end{bmatrix}, \tag{4}$$

and tensor S can be written as:

$$S = \begin{bmatrix} S_{11}^{E} & S_{12}^{E} & S_{13}^{E} & 0 & 0 & 0 \\ S_{12}^{E} & S_{22}^{E} & S_{23}^{E} & 0 & 0 & 0 \\ S_{13}^{E} & S_{23}^{E} & S_{33}^{E} & 0 & 0 & 0 \\ 0 & 0 & 0 & S_{44}^{E} & 0 & 0 \\ 0 & 0 & 0 & 0 & S_{55}^{E} & 0 \\ 0 & 0 & 0 & 0 & 0 & 2\left(S_{11}^{E} - S_{12}^{E}\right) \end{bmatrix} \tag{5}$$

A mechanical vibration sensor can be modeled by a mass-spring-damper system. Considering the mass-spring-damper system of Fig. 3 with mass m, elasticity constant k and damping coefficient b, in the referential $u(t)$, which is an accelerated referential, there are several forces acting on the sensor, as it is shown in Fig. 3.

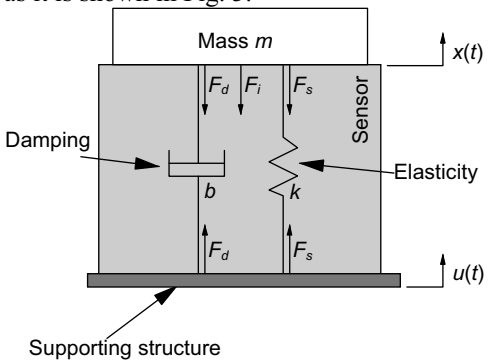

Fig.3. Mechanical structure of the sensor, which can be modeled as a damper and a spring.

Nevertheless, the resultant of these forces is only the reaction to an inertial force that acts in mass m, which results from the fact that $u(t)$ is an accelerated referential. This force is given by:

$$F_i = -m\frac{d^2u(t)}{dt^2}. \tag{6}$$

Considering the approximation that the sensor has exactly the same strain as the mass m and knowing that the force

acting on it is applied in the direction 3, the polarization of the piezoelectric material is:

$$P(t) = d_{33}\sigma_3 = \frac{d_{33}F_i}{A} = -\frac{m\,d_{33}}{A}\frac{d^2u(t)}{dt^2}, \quad (7)$$

where A is the area of the electrodes of the sensor. Considering that the polarization is uniform in all the sensor area, this polarization corresponds to an electrical charge of:

$$Q(t) = \iint P(t)\,dx\,dy = A\,P(t) = -m\,d_{33}\frac{d^2u(t)}{dt^2}, \quad (8)$$

and the output voltage of the sensor is:

$$v(t) = \frac{Q(t)}{C(t)} = \frac{-m\,d_{33}\,x(t)}{\chi_{33}^{\sigma}A}\frac{d^2u(t)}{dt^2}, \quad (9)$$

where $C(t)$ is the capacitance of the sensor, which changes in time with the force F_i.

By the other hand, the value of $x(t)$ can be obtained from:

$$x(t) = t_s\left(1+\varepsilon_3\right) \quad (10)$$

where t_s is the thickness of the sensor at the steady state. ε_3 is given by:

$$\varepsilon_3 = s_{33}^{E}\sigma_3 = s_{33}^{E}\frac{F_i}{A}. \quad (11)$$

With the piezoelectric element working in its linear region, ε_3 is several orders of magnitude lower than 1, so it can be disregarded and eq. (9) can be simplified to:

$$v(t) = \frac{-m\,d_{33}\,t_s}{\varepsilon_o\varepsilon_r A}\frac{d^2u(t)}{dt^2}, \quad (12)$$

Calculating the Laplace transform of both members of eq. (12) gives:

$$V(s) = \frac{-m\,d_{33}t_s}{\varepsilon_o\varepsilon_r A}s^2U(s). \quad (13)$$

The transfer function of the system is:

$$G(s) = \frac{V(s)}{U(s)} = \frac{-m\,d_{33}t_s}{\varepsilon_o\varepsilon_r A}s^2 \quad (14)$$

In order to simplify the model, another assumption was made: The sensor is small enough that no modal sensing comes to effect. In other words, the strain is uniformly distributed over the sensor area.

Fig. 4 shows the electric equivalent model of a piezoelectric sensor. It can be modeled as a current source in parallel with a capacitor.

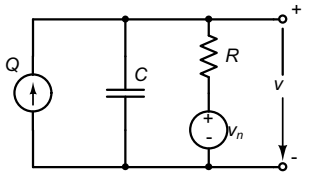

Fig. 4. Equivalent circuit of a piezoelectric sensor [10].

A resistor and a voltage source are included too to represent the leakage of the charges generated by the sensor and the noise sources. From this model, the noise transfer function can be calculated, giving [10]:

$$G_n(s) = \frac{V(s)}{V_n(s)} = \frac{1}{1-sRC} \quad (15)$$

By analyzing eq. (14) and eq. (15) it is possible to conclude that the piezoelectric sensor has the behavior of a high-pass filter to the input signal $\left(u(t)\right)$ and behaves like a low-pass filter for the generated noise. Both cases prove that the sensor has a superior performance at high frequencies.

A. Seismic sensor design considerations

The parameters that must be set by the sensor designer are the mass m, the sensor area A and the sensor thickness t. Nevertheless, the sensor always shows a high-pass response. As it was referred in a previous section of this article, electrostatic and electromagnetic transducers could also be used. Our choice fell on the piezoelectric transducers due to the disadvantages presented by the other two technologies: the theoretical sensibility of the electrostatic transducers is about ten times lower than the one of the piezoelectrics [5, 6] and with the electromagnetic transducers it is difficult to reach the operation frequency range purposed in this work.

Table 1 shows some piezoelectric parameters of β-PVDF.

TABLE I
PIEZOELECTRIC PARAMETERS OF Β-PVDF.

Parameter	Value
d_{33}	$-35\times10^{-12}\ mV^{-1}$
s_{33}	$4.72\times10^{-12}\ m^2N^{-1}$
ε_r	12

Fig. 5 shows the frequency response of the sensor coupled to a mass $m = 18$ g. The sensor area is 2.25 cm^2 and its thickness is 90 μm.

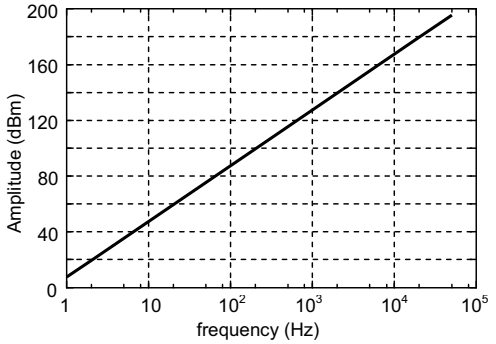

Fig. 5. Frequency response of the sensor attached to a mass of 18 g. The sensor area is 2.25 cm^2 and its thickness is 90 μm.

IV. FABRICATION OF THE SENSOR

A. Polymer preparation

The piezoelectric film used as sensor is constituted by a polymeric material coated in both sides by a conducting material, which forms the electrodes. The polymeric material is based on the poly(vinylidene fluoride) (PVDF) polymer in its electroactive β phase. It can be processed in the form of a film by extrusion, injection or from the solution, usually in the non electroactive α phase. A method to obtain the electroactive β phase from α phase films consists in submitting them to mechanical stretching at temperatures below 100ºC and with a stretching ratio (ratio between the final and the initial lengths of the sample) from 4 to 7.

Nevertheless, for the present work, high performance films, prepared by a method patented by us have been used [7, 8]. Unoriented films exclusively in the β phase were obtained from the crystallization of PVDF from solution with N,N-Dimethyl Formamide or Dimethyl Acetamide at temperatures below 70 C. The electromechanical properties of the film were improved by a treatment that consists on pressing, stretching and poling at high temperature [7]. A final step of stretching at a temperature around 80ºC results in oriented films, which further increases the material performance. Final film thickness ranged from 20 μm to 60 μm.

B. Electrode deposition

Once the piezoelectric material is prepared, electrodes are deposited on both sides either by magnetron sputtering or by thermal evaporation. Aluminum has been used as electrode material for the present work.

The thermal deposition system consists in a vacuum chamber where the pressure reaches 10^{-6} mbar. An evaporation boat containing the material to be evaporated is placed in its interior. The boat is heated by means of an electric current ranging between 100 A and 200 A. At the top of the chamber the β-PVDF film, where the deposition is performed, and one mass sensor are placed. In order to deposit the electrode on the thin β-PVDF polymer, the electrical power applied to the boat must increase slowly. When the temperature of evaporation of the Aluminum is reached, the mass sensor will indicate a variation of the mass attached to it - proportional to the film thickness. At this point, the electrical power must be kept constant. When the mass sensor indicates that the electrode thickness is equal to 30 nm, the power supply is switched off and the deposition of the electrode is complete. The second electrode is deposited by turning upside down the β-PVDF film and repeating the previous procedure. Fig. 6 shows a picture of the sensor obtained after these fabrication steps.

Fig. 6. Picture of the sensor element.

V. READOUT ELECTRONICS

The sensor absorbs the seismic waves and generates an electrical voltage according to their amplitudes and frequencies. As the amplitude of the vibrations to be measured is very small, the obtained electrical voltage obtained at the sensor terminals is also small, so, an amplification stage is required. The amplifier is based in the Burr-Brown INA114, which is a monolithic precision instrumentation amplifier [9]. It has very high input impedances, both in the differential mode between the two input terminals as well as in the common mode between each of the input terminals and earth. It has low output impedance being a bit sensitive to the output load downstream. The common-mode rejection ratio (CMRR) is very high, being the output voltage essentially proportional to the voltage difference between the two inputs.

Finally, the piezoelectric element is placed inside a metallic box that works as a Faraday cage, avoiding the interferences caused by electromagnetic radiations. Fig. 7 shows the sensor and the amplifier.

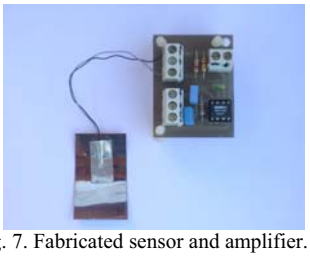

Fig. 7. Fabricated sensor and amplifier.

In order to acquire the data coming from the sensor, the National Instruments NI-USB-9201 data acquisition board was used, which has a sample rate of 500 kS/s, a resolution of 12 bits and a maximum voltage range from -10 V to10 V.

In order to observe and process the data collected by the data acquisition board, it was created a virtual instrument using the LabVIEW from National Instruments as the programming language.

Fig. 8 shows the user interface of the virtual instrument. This interface allows the user to observe the propagation of waves in real time (graph of the top of Fig. 8). It also allows the storing of the collected data for further use. The collected data are recorded in a file and is displayed in the virtual instrument panel (graph of the bottom of Fig. 8). From the stored data it is possible to know the positive peak voltage, the negative peak voltage, the peak to peak voltage and the rms (root mean square) value of the data that lies in a specified interval.

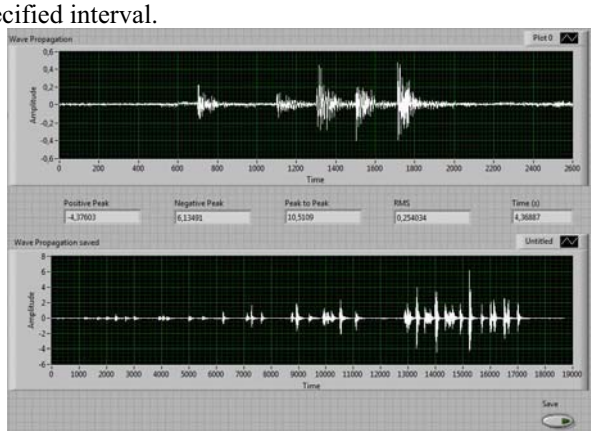

Fig. 8. Visual aspect of the virtual instrument created with LabVIEW.

The first and simplest test was performed by placing the sensor on the floor. Then, a person kicked the floor near the sensor. Fig. 9 shows the obtained waveform obtained for two consecutive kicks.

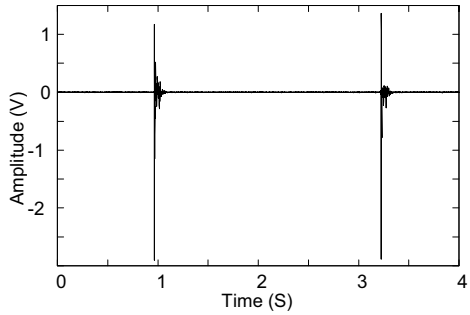

Fig. 9. Waveform obtained with the sensor when a person kicks the floor. The sensor was placed on the floor at a distance of approximately 3 m from the point where the person kicked.

In the second test, the sensor inside the box was coupled to a shaker that can vibrate at frequencies up to 500 Hz. Fig. 10 shows the spectral response obtained in this test. This result is in pretty good accordance with the frequency response plotted in Fig. 5.

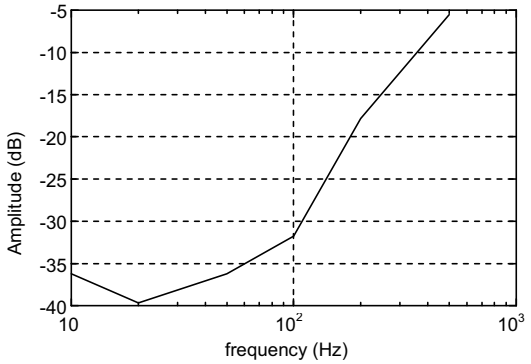

Fig. 10. Spectral response obtained with the sensor inside the box coupled to a shaker.

Once the sensor is constructed, the sensor was tested under a real environment. This test consisted in the placement of the sensor near a stone-quarry, where explosions are used to extract the stones. Figs. 11 to 13 show some of the obtained waveforms.

Fig. 11 shows the waveforms obtained in the first explosion.

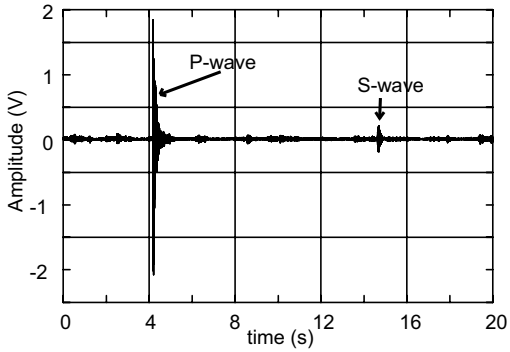

Fig. 11. Waveforms obtained from an explosion consisting in two simultaneous shots. One of them occurred at a depth of 3.10 m with 2 kg of gunpowder, while the other occurred at a depth of 2.40 m with 1.125 kg of gunpowder.

In this explosion, two simultaneous shots occurred. One of them occurred at a depth of 3.10 m with 2 kg of gunpowder, while the other occurred at a depth of 2.40 m with 1.125 kg of gunpowder. As it can be seen in the figure, it is very difficult to identify the two shots. A detailed analysis of the results show that the time arrival difference between the two vibrations is less than 40 ms. Nevertheless, it is very clear in the figure the arrival of the primary and secondary waves.

The second explosion consisted in a single shot caused by 0.44 kg at a depth of 1.6 m. The result is represented in Fig. 12.

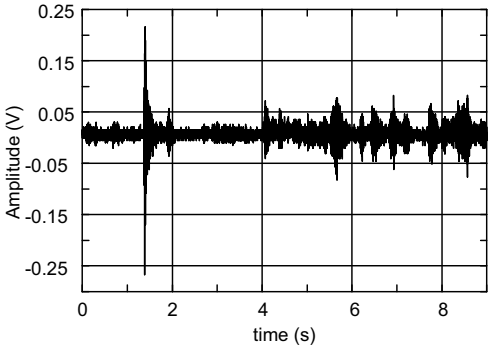

Fig. 12. Result of an explosion consisting in a single shot caused by 0.44 kg of gunpowder at a depth of 1.6 m.

The last explosion consisted in a single shot of 88 g of gunpowder at a depth of 0.7 m, in a free stone block. The results are presented in Fig. 13.

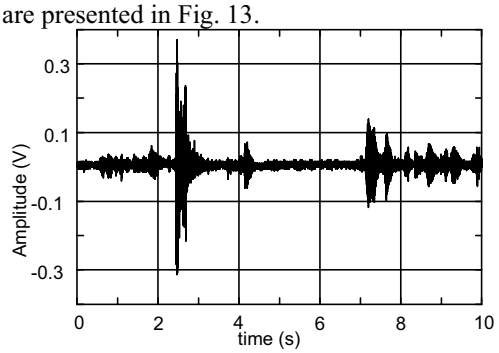

Fig. 13. Result of an explosion consisting in a single shot of 88 g of gunpowder at a depth of 0.7 m, in a free stone block.

After the observation of the signals of Figs. 11, 12 and 13, it is possible to see two main differences between the signals produced by the explosions in fixed blocks (Figs. 11 and 12) and the signal produced by the explosion in the free block (Fig. 13). The amplitude of the signal obtained from the free block is lower than the others and has several peaks in a 350 ms interval. The peaks of the signals that came from the fixed blocks decreased exponentially during approximately 100 ms.

VI. Conclusion

The fabrication steps of a seismic sensor based on a piezoelectric poly(vinilidene fluoride) –PVDF- polymer film has been presented. The lightness, sensitivity, wide frequency piezoelectric response and mechanical characteristic of this material make it suitable for detecting the amplitudes and frequencies characteristic of seismic events. Further, if needed the characteristics of the material can be fine tuned in order to match characteristics for a given application. The

sensor is low cost an easy to fabricate. The readout electronics and software mediated data acquisition system allow an easy test implementation of the sensor in real environments where seismic vibrations can take place or can be simulated. This will be the next step of the present project. As a future work, the sensor will be placed in a seismic station located at the Azores islands, where the seismic activity is very intense. The main objective will be to detect and characterize high frequency vibrations.

ACKNOWLEDGEMENTS

The authors thank the Portuguese Foundation for Science and Technology – FCT (Grant PTDC/CTM/69362/2006) for financial support.

REFERENCES

[1] Dytran Seismic sensor model 3191A Data Sheet, Dytran Instruments,Inc.
[2] Ultra-sound theory- http://www.forp.usp.br/restauradora/us01.htm
[3] Piezoelectric theory - http://americanpiezo.com/piezo_theory/
[4] Piezoelectric transducers theory - http://www.ndt-ed.org/EducationResources/CommunityCollege/Ultrasonics/EquipmentTrans/piezotransducers.htm.
[5] S. Roundy, P.K. Wright, and J. Rabaey, "Energy Scavenging for Wireless Sensor Networks with Special Focus on Vibrations," Kluwer *Academic Press*, 2003.
[6] S. Roundy, E. S. Leland, J. Baker, E. Carleton, E. Reilly, E. Lai, B. Otis, J. M. Rabaey and P. K. Wright, "Improving Power Output for Vibration-Based Energy Scavengers," *IEEE Pervasive Computing*, Vol. 4, 2005, pp 28-36.
[7] V. Sencadas, R. Gregorio Filho and S. Lanceros-Mendez, "Processing and characterization of a novel nonporous poly(vinylidene fluoride) films in the beta phase," *J. Non-Crystalline Solids*, V. 352, 2006, pp. 2226-2229.
[8] S. Lanceros-Mendez, V. Sencadas and R. Gregorio Filho "Non-Porous Polyvinylidene Fluoride (Pvdf) Films In The Beta Phase And Processing Method Thereof," Patent WO2007010491, 2006.
[9] Instrumentation Amplifier Datasheet – http://focus.ti.com/lit/ds/symlink/ina114.pdf
[10] S. Kon, and R. Horowitz "A High-Resolution MEMS Piezoelectric Strain Sensor for Structural Vibration Detection," *IEEE Sensors J*., Vol. 8, No. 12, 2008, pp. 2027-2035.